Paper No. 456. (quote when citing this article)
Eleventh World Conference on Earthquake Engineering
ISBN: 0 08 042822 3

SHAKING TABLE TESTS OF EARTHQUAKE RESISTING WALLS

SHUICHI YABANA, KENJI KANAZAWA,

Central Research Institute of Electric Power Industry
1646, Abiko, Abiko-shi, Chiba-ken, 270-11, JAPAN
Phone: +81 471 82 1181 Fax: +81 471 83 2962
e-mail yabana@abiko.denken.or.jp

YUKIO OHMIYA, HAJIME TANIGUCHI and ATSUSHI KAMBAYASHI

Takenaka Corporation
8-21-1, Ginza, Chuo-ku, Tokyo, 104, JAPAN
Phone: +81 3 3542 7100 Fax: +81 3 3545 0974

ABSTRACT

In this paper, results of dynamic tests on reinforced concrete (RC) earthquake resisting walls with a shaking table were described. Four same test specimens were prepared to obtain behavior of the walls under different excitations which were sine sweep waves and simulated seismic waves. The ultimate response and the nonlinear characteristics of the walls were obtained from the test results. In particular, it was found that the damping of the walls varied with its damage and cyclic loadings. Furthermore, an analytical model of RC earthquake resisting walls for FEM was developed to calculate the ultimate response and it was verified by application to the shaking table tests.

KEYWORDS

Earthquake resisting walls; reinforced concrete; shaking table tests; dynamic nonlinear characteristics; dynamic failure; 3D FEM; nonlinear analysis; layered shell elements; constitutive models.

INTRODUCTION

In order to investigate the safety of a box-frame type RC structure such as a nuclear power building against seismic loads, it is important to make clear the dynamic nonlinear characteristics of RC earthquake resisting walls. Although a lot of static tests on earthquake resisting walls have been carried out to obtain the nonlinear characteristics, few dynamic tests were carried out. On the other hand, an accurate analytical model for RC resisting walls is necessary to calculate the safety margin of the structures.

In this paper, results of dynamic tests on RC earthquake resisting walls with a shaking table were mentioned. Furthermore, an analytical model of RC earthquake resisting walls for FEM was developed and verified by application to the shaking table tests.

SHAKING TABLE TESTS

Test Specimens

A test specimen of an earthquake resisting wall is shown in Fig. 1 and Fig. 2. Four same test specimens were prepared to obtain behavior of the walls under different excitations. These test specimens were called Specimen A, B, C and D. The thickness and height of the walls were 4 cm and 80 cm, respectively. The length of the walls in excited direction was 100 cm. Deformed bar of diameter 6 mm and mortal were used in the walls of the test specimens and reinforcement ratio was 1 %. Leaden weights were mounted on the top

specimen had high natural frequency, the simulated seismic wave in real time scale would not cause failure. Thus time scale of the simulated seismic waves reduced to 1/4 or 2/5 of original ones to do larger damage to test specimens. The former was called Wave-1 and the latter was called Wave-2. Specimen C was subjected to Wave-1 and Specimen D was subjected to Wave-2. The accelerogram and the response spectrum of Wave-2 are shown in Fig. 4 and Fig. 5. Specimen C and D were subjected to a sine sweep waves finally.

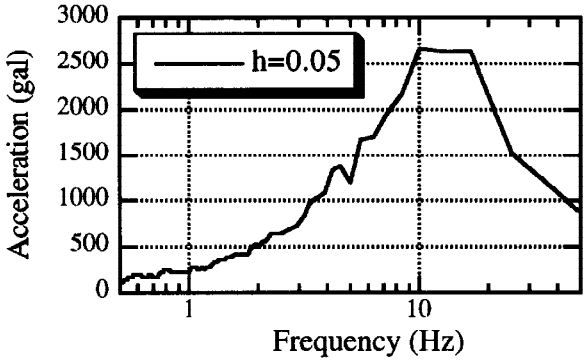

Fig. 5 Response spectra of Wave-2

Results of Shaking Table Tests

Maximum response values in principal excitations are shown in Table 2. Maximum response acceleration in both horizontal and vertical directions increased with increase of input acceleration. In particular, vertical acceleration at the upper slab was remarkably excited by large input acceleration. In the case of excitation No. B-18 and D-16, shear force reached the maximum shear strength of the walls. Furthermore, a lot of cracking failures and fall of concrete pieces were observed at the same time. The maximum shear strength of the walls was about 33 tonf, which was calculated with maximum acceleration. The maximum deformation angle was 8×10^{-3} in the final excitation.

Table 2 Maximum response values in principal excitations

	Specimen B			Specimen D	
No. of Excitation	B-14	B-16	B-18	D-14	D-16
Input Wave	Sine Sweep (24-16 Hz)	Sine Sweep (18-12 Hz)	Sine Sweep (15-10 Hz)	Wave-2	Sine Sweep (15-10 Hz)
Max. Input Acc. on the Table	726gal	676gal	819gal	1039gal	951gal
Max. Horizontal Acc. on the Foundation Slab	699gal	824gal	977gal	1017gal	1409gal
Max. Horizontal Acc. at the Upper Slab	1376gal	2347gal	2619gal	2056gal	2748gal
Max. Vertical Acc. at the Upper Slab	3069gal	5589gal	6809gal	4023gal	7727gal
Max. Deformation Angle	1.8×10^{-3}	5.0×10^{-3}	7.9×10^{-3}	3.4×10^{-3}	8.3×10^{-3}
Max. Shear Force	17.0tf	29.0tf	32.3tf	25.4tf	33.9tf

Stiffness and damping factor after each excitation were estimated by system identification using the ARMA model. Relation between the parameters are shown in Fig. 6. Initial natural frequency of the test specimen was about 30 Hz. Stiffness of the walls after the failure reduced to about 1/5 of their initial stiffness. Damping factor increased with the damage and it varied from 0.02 to about 0.2. Stiffness and damping factor of Specimen A and B subjected to almost same excitations similarly varied, so that the characteristics of test specimens might be almost same. The variation of the parameter of Specimen C was different from one of Specimen D, because of difference damage given by Wave-1 and Wave-2.

Variation of equivalent damping factor during the excitation was calculated every half cycle of a hysteresis loop as shown in Fig. 7. The time histories of equivalent damping factor and relative displacement at the upper slab in the case of D-14 and D-16 are shown in Fig. 8. In D-14 subjected to Wave-2, equivalent damping factors randomly varied and showed a little tendency to increase as time went on.

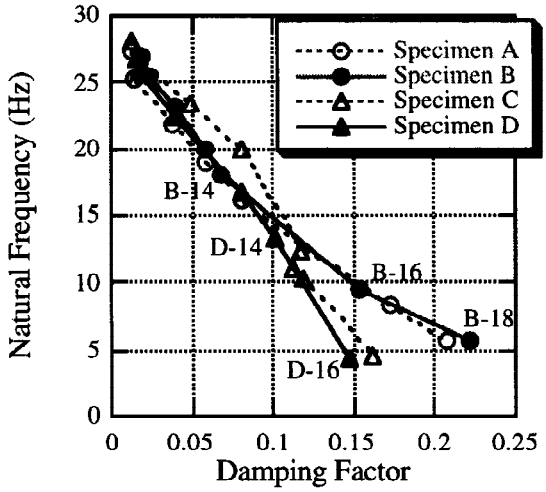

Fig. 6 Relation between stiffness and damping factor after each excitation

On the other hand, these factors transiently increased with increase of relative displacement and reduced under constant amplitude of dynamic cyclic loading in D-16 subjected to the sine sweep wave after 0.4 second. From the result, it was found that equivalent damping factor reduced under constant amplitude of the dynamic cyclic loadings. Moreover, it might be efficient to evaluate an analytical model with the variation of damping factor during excitations.

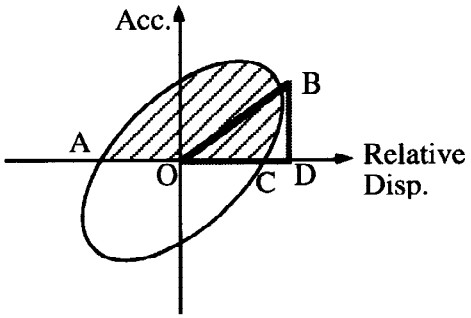

Equivalent damping factor $h = \frac{1}{2\pi} \frac{\Delta ABC}{\Delta OBD}$

Fig. 7 Calculation method for equivalent damping factor during 1/2 loop

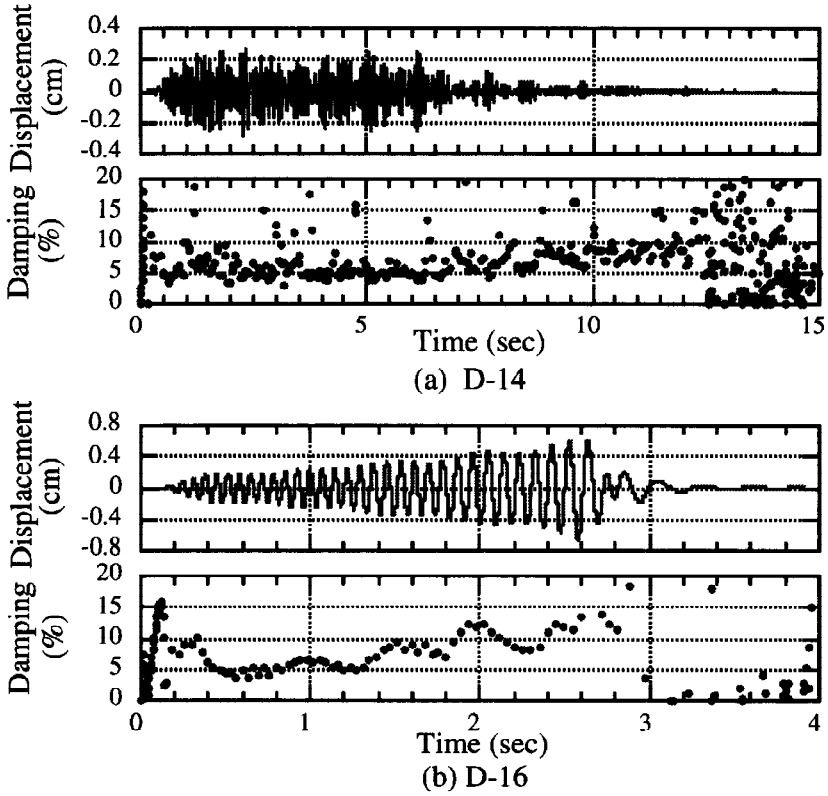

Fig.8 Relative displacement and equivalent damping factor every half cycle of hysteresis loops

Relations between relative displacement and acceleration at the upper slab in D-14 and D-16 are shown in Fig. 9. These figure can be approximately regarded as relations between relative displacement and restoring force. It was found that hysteretic damping radically increased after shear stress reached maximum strength in comparison with these figures. Then the stiffness decreased after that and failure of the test specimen occurred in D-16 finally.

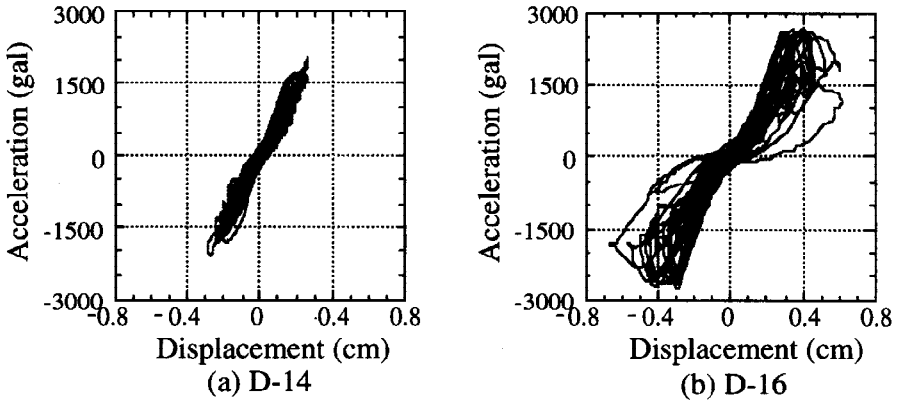

Fig. 9 Relation between relative displacement and acceleration at upper slab

Final crack pattern of the Specimen D are shown in Fig. 10. It was found that the failure was typical shear failure from the final crack pattern. Maximum tensile strain of reinforcing bars of the Specimen D are shown in Fig. 11. The arrows in Fig. 11 show maximum tensile strain and its direction at each point and circles mean the yielding strain of the bars. Although the bars hardly yielded in D-14, while some bars did due to the failure of the wall in D-16. The tensile strain at the lower part of the wall was larger than one at the upper part because of rocking vibration. Furthermore, the strain became larger at the failure part where concrete pieces fell.

Fig. 10 Final crack pattern of test specimen D

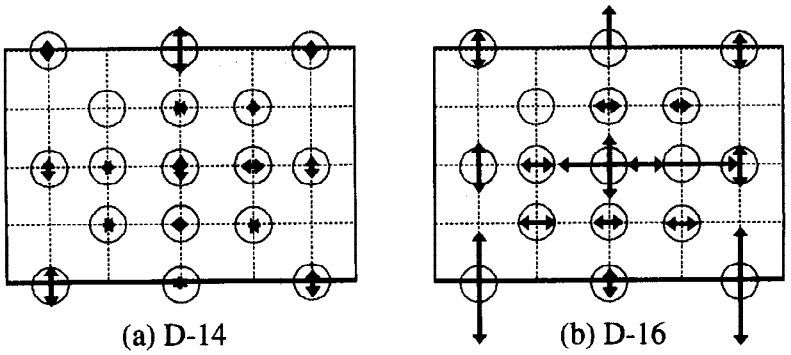

(a) D-14 (b) D-16

Fig. 11 Distribution of tensile strain of test specimen D

SIMULATION

Analytical Moels for RC Earthquake Resisting Walls

FEM model of the specimen is shown in Fig. 12. The analytical model was the upper part of the foundation slab and 1/2 model in consideration of the symmetry of the test specimens. The upper slab was composed of linear shell elements and the walls were modeled by layered shell elements to consider the material non-linearity of concrete and reinforced bars as shown in Fig. 13. The leaden weights on the upper slab was uniformly distributed on the shell elements.

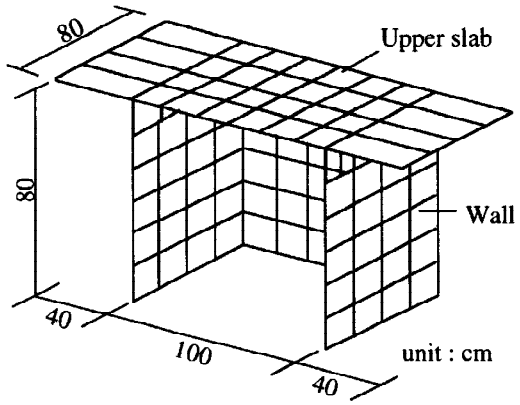

Fig. 12 FEM model of the test specimen

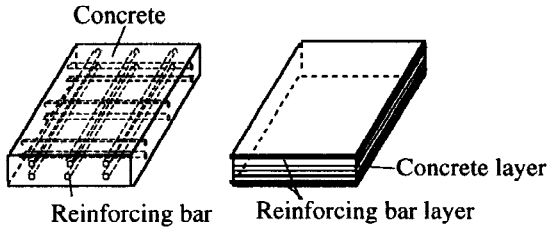

Fig. 13 Outline of layerd shell element

Constitutive Models for RC Walls

The layered shell elements consisted of 4 concrete layers and 2 reinforcing bar layers. In each concrete layer the material nonlinearity was considered. The nonlinear model for concrete prior to cracking was assumed to be elasto-plastic based on Drucker - Prager's yielding criteria. The constitutive model of concrete after cracking was based on a smeared crack model. The cracking was evaluated from maximum principal stress. A secondary crack under cyclic loadings was assumed to appear in the normal direction of the existing crack. The stress-strain relationship for cracked concrete was assumed as Eq. 1, which was defined by rectangular coordinate system to the crack plane as shown in Fig. 14.

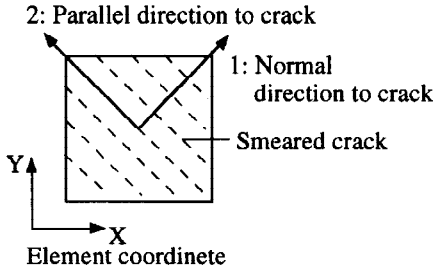

Fig. 14 Coordinete system after cracking

$$\begin{Bmatrix} \Delta\sigma_1 \\ \Delta\sigma_2 \\ \Delta\tau_{12} \end{Bmatrix} = \begin{bmatrix} E_1(\varepsilon_1) & 0 & 0 \\ 0 & E_2(\varepsilon_2) & 0 \\ 0 & 0 & G_{12}(\varepsilon_1,\varepsilon_2) \end{bmatrix} \begin{Bmatrix} \Delta\varepsilon_1 \\ \Delta\varepsilon_2 \\ \Delta\gamma_{12} \end{Bmatrix} \quad (1)$$

where, σ_1, ε_1 : Stress and strain normal to a crack plane

σ_2, ε_2 : Stress and strain parallel to a crack plane

τ_{12}, γ_{12} : Shear stress and strain.

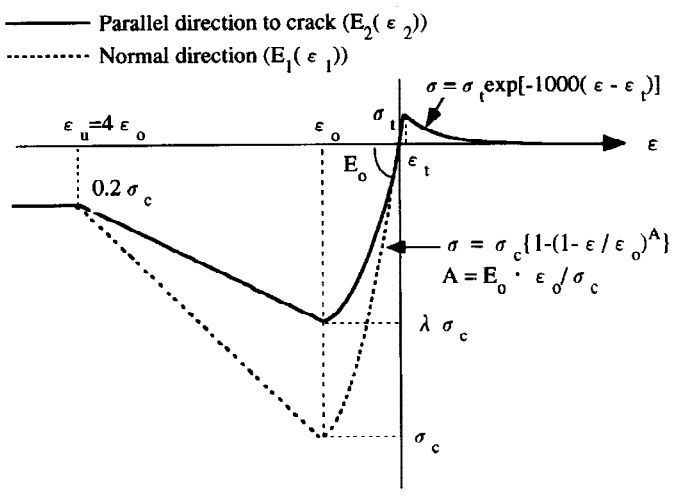

Fig.15 Envelop curve of stress-strain relationship of concrete

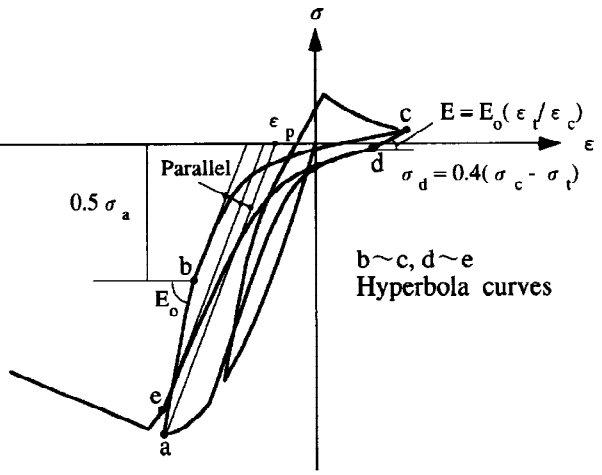

Fig.16 Stress-strain relationship of concrete under cyclic loadings

The envelope curves of the stress-strain relationship model normal and parallel to the crack plane ($E_1(\varepsilon_1)$ and $E_2(\varepsilon_2)$) are shown in Fig. 15. The compressive stress-strain relationship model until the maximum compressive strength was based on the model proposed by Fafitis and Shah (1985). Then the model in tensile state of concrete was developed with Collins' model (Stevens, I.D. *et al..*, 1987), taking account of the tension-stiffening effect. After cracking, the compressive strength and stiffness parallel to the crack plane were assumed to be proportionally reduced in the ratio λ. The hysteresis curves under cyclic loadings were composed of hyperbola curves and straight lines as shown in Fig. 16. The curves connected experienced maximum strains in both compression and tension The curves in the compressive region were modeled on the plastic strain ε_p (Karsan *et al.*, 1969). Furthermore, the deterioration of concrete strength by cyclic loadings were considered with the equation proposed by Yamada *et al.* (1977). The interface shear stiffness model with respect to a crack plain ($G_{12}(\varepsilon_1,\varepsilon_2)$) was assumed as shown in Fig. 17 (Yamada *et al.*, 1983).

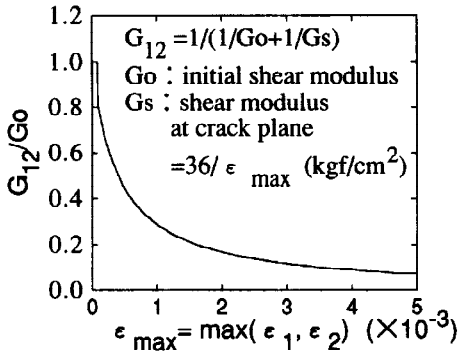

Fig. 17 Shear rigidity after cracking

The reinforcing bars were represented by anisotropic steel plates with equivalent thickness to the cross sectional area. The nonlinearity of the bars was used bilinear model.

Table 3 Material properties of the mortal for the simulations

	Specimen B	Specimen D
Compressive strength : σ c (kgf/cm^2)	315	340
Young's modulus : Eo ($\times 10^5$kgf/cm^2)	2.07	2.20
Strain at maximum strength: ε o ($\times 10^{-3}$)	2.75	
Tensile strength : σ t (kgf/cm^2)	15	
Reduction coefficient : λ	0.62	0.61

Method and Condition of Numerical Analysis

Newmark's β method (β = 1/4) was used as numerical integration to calculate the response of the walls. Newton - Raphson method was employed in nonlinear analysis. Stiffness proportional damping was assumed and damping factors was changed from 0.005 to 0.015, taking account of stiffness reduced by the damage of the wall. Each simulation was analyzed with final stress and crack in previous simulation. Material properties of the mortal for the simulations were shown in Table 3.

Analytical Results

Fig. 18 shows time histories of the tests and the analyses in excitation No. B-16, D-14 and D-16 for comparison. In the case of B-16 and D-14, the analytical results agreed well with the test results. Since failure of the test specimen occurred in D-16, analytical results did not show good agreement with the test results after 2 second.

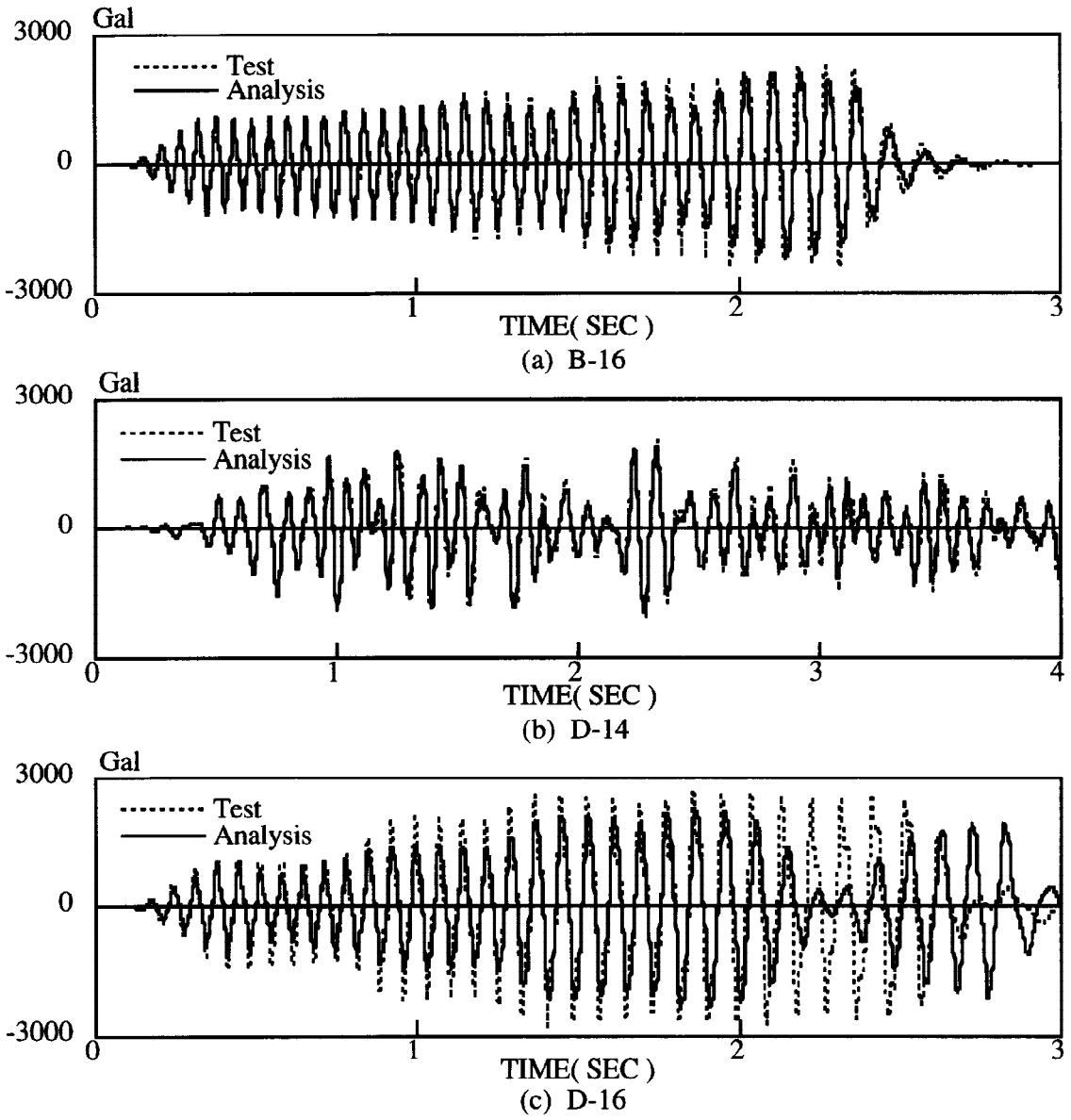

Fig.18 Comparison of response accelerations at the upper slab in the tests with analytical results

Relations between relative displacement and acceleration at the upper slab are shown in Fig. 19. The hysteresis loops of the analyses were similar to the test results and maximum displacements of the analyses agreed with one of the tests except for D-16.

From the above results, the proposed analytical model was confirmed the validity except for drastic failure of RC structures.

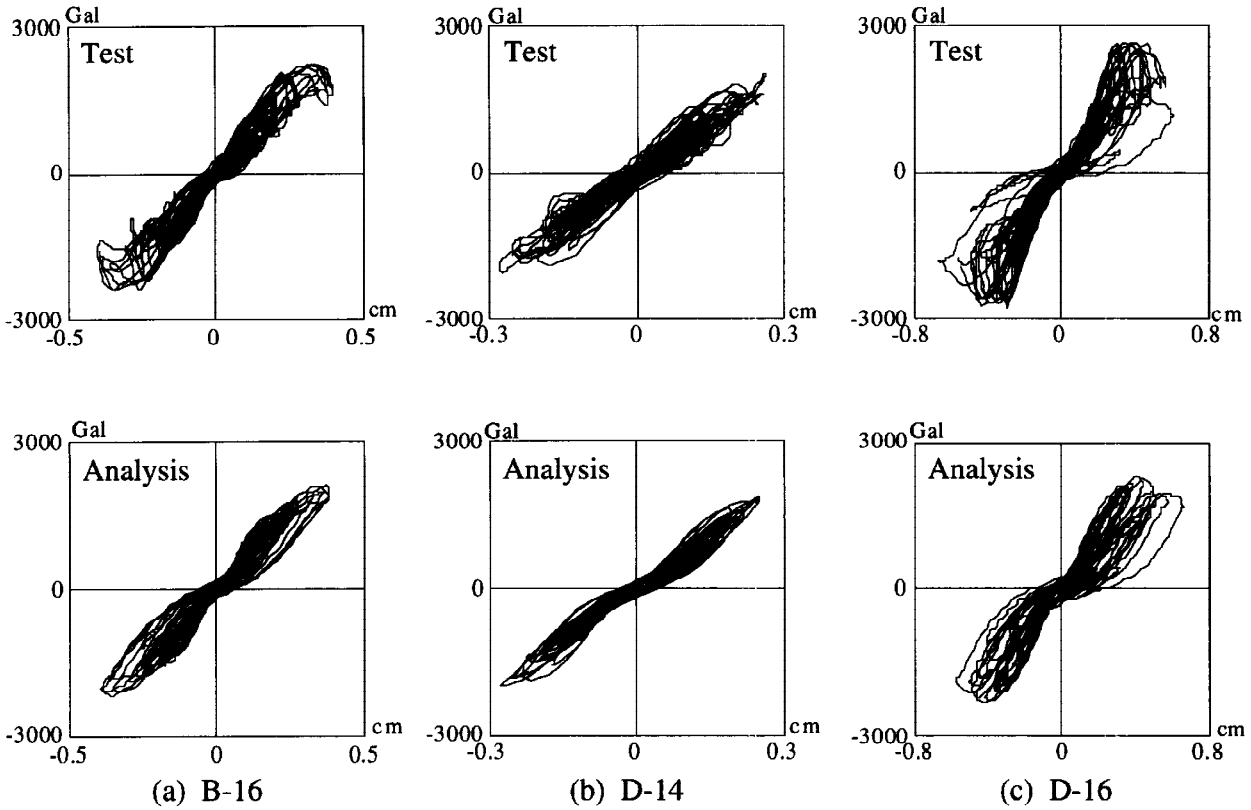

Fig.19 Comparison of hysteresis loops in the tests with analytical results

CONCLUSIONS

This paper was described about shaking table tests of RC resisting walls and its simulation with FEM developed by the authors.

Significant data on dynamic nonlinear characteristics and failure of the RC earthquake resisting walls were derived from the tests. In particular, it was found that equivalent damping factor reduces under constant amplitude of dynamic cyclic loadings.

The analytical model of RC walls for FEM to calculate the ultimate response was verified by application to the shaking table tests. The FEM analysis with the analytical model is effective for analyses of seismic margin of RC structures.

REFERENCES

Fafitis, A. and Shah, S. P. (1985) . Lateral Reinforcement for High-Strength Concrete Columns, *ACI Special Publication, No. SP-87,* pp. 213 - 232.

Stevens, I.D., Uzumeri, S.M. and Collins, M.P. (1987). Analytical Modeling of Concrete Subjected to Monotonic and Reversed Loadings. *Department of Civil Engineering, Publication No.87-1,* University of Toronto.

Yamada and Aoyagi (1983). Shear transfer model for cracking faces. Conference on Shear of Concrete in Analytical Study. (in Japanese)

Yamada, M., Kawamura, H. and Morishita, H. (1977). Study on plastic fatigue of concrete. Summaries of Technical Papers in Kinki Area, Architectural Institute of Japan. pp. 21 - 24. (in Japanese)

Karsan, I.D. and Jirsa, J.O. (1969). Behavior of concrete under compressive loading. *Journal of Structural Division, ASCE, 12,* pp. 2543 - 2563.